Novel androgen-induced activity of an antimicrobial b-defensin: Regulation of Wolffian duct morphogenesis

Novel androgen-induced activity of an antimicrobial β-defensin:

regulation of Wolffian duct morphogenesis

Camilla M. Ribeiro[1], Lucas G. A. Ferreira[1], Daniel S. Thimoteo[1], Lee B. Smith[2], Barry T. Hinton[3],

5   Maria Christina W. Avellar[1]*

[1]Section of Experimental Endocrinology, Department of Pharmacology, Universidade Federal de São Paulo – Escola Paulista de Medicina, São Paulo, SP, Brazil. [2]MRC Centre for Reproductive Health, University of Edinburgh, The Queen's Medical Research Institute, Edinburgh, UK. [3]Department of Cell

10   Biology, University of Virginia, School of Medicine, Charlottesville, Virginia, USA.

*Correspondence should be addressed to: Maria Christina W. Avellar, Section of Experimental Endocrinology, Department of Pharmacology, Universidade Federal de São Paulo, Escola Paulista de Medicina, Rua 03 de maio 100, INFAR, Vila Clementino, São Paulo, SP, Brazil, 04044-020. Email:

15   avellar@unifesp.br. Phone/Fax: (55) (11) 5576-4448.

ABSTRACT

The Wolffian duct (WD) undergoes morphological changes induced by androgens to form the epididymis, which is an organ essential for sperm maturation. Androgen action in WD epithelium involves paracrine factors of mesenchymal origin that function by still poorly understood mechanisms. Here we studied the antimicrobial β-defensin SPAG11C as a new player in duct morphogenesis, localized prenatally in the WD mesenchyme. Organotypic culture of rat WDs and tissues from Androgen Receptor (AR) knockout mice (ARKO) were used. Our results show that androgen/AR signaling differentially regulated SPAG11C expression at mRNA and protein levels in the developing WD. WDs incubated with recombinant human SPAG11C were shorter and less coiled as a result of reduced epithelial cell proliferation, but not increased apoptosis. Our results suggested β-defensin SPAG11C as an androgen-target required for WD morphogenesis. This highlights the multifunctional repertoire of the β-defensin protein family and their potential contribution to the *in utero* environment that determines male reproductive success.

KEYWORDS: Wolffian duct, male infertility, androgen, epididymis, β-defensin, innate immunity

1. INTRODUCTION

Tubular morphogenesis is a fundamental process during the development of the male urogenital tract. The morphological changes observed during the embryonic development of the Wolffian duct (WD), the precursor of the epididymis, transform a straight duct into a three-dimensionally long, coiled and regionalized structure. Disruption of the events by which WD elongates and coils in utero may result in abnormal epididymal shape and length that later, in adulthood, can compromise sperm maturation and therefore male fertility (Murashima et al., 2015b).

Inhibin beta A (Tomaszewski et al., 2007), growth factors (Gupta, 1996; Kitagaki et al., 2011, Okazawa et al., 2015) and members of the Wnt pathway (Carrol et al., 2005; Kumar et al., 2016) have been shown important regulators of WD morphogenesis. Although cell proliferation is required for elongation, cell rearrangements regulated by protein tyrosine kinase 7 is also a major driver of WD elongation (Hinton et al., 2011; Xu et al., 2016). During very early development of the WD, androgens are essential for the stabilization of the duct in male embryos and later are also needed for the subsequent differentiation of the WD into the epididymis (Welsh et al., 2007, 2008; Murashima et al., 2011). Testosterone, but not its metabolite dihydrotestosterone (DHT), plays a dominant role in these processes (Tsuji et al., 1991; Imperato-McGinley et al., 1992; Murashima et al., 2015a) through the activation of the androgen receptor (AR), a member of the nuclear receptor superfamily. Different experimental approaches, including the use of pharmacological tools and genetic models, demonstrated that androgen action during WD morphogenesis involves dynamic mesenchymal-epithelial interactions under the control of AR signaling that drives androgen-dependent mesenchyme-derived molecules that act as WD epithelial paracrine regulators (Hannema et al., 2006; Archambeault et al, 2009; Welsh et al., 2009; Murashima et al., 2011). However, little is known about the cellular mechanisms involved in the complex interplay of modulatory factors driven by androgen signaling during WD morphogenesis.

Recently we reported that the *Spag11c* gene (sperm-associated antigen 11), a member of the β-

defensin family of epithelial antimicrobial peptides, drastically changes its expression pattern as the rat epididymis develops from prenatal to postnatal life (Ribeiro et al., 2015). We showed that the *Spag11c* mRNA, detected as early as in the embryonic age (e) e12.5 in the rat WD, transiently increased in its abundance at e17.5 and then decreased at e20.5, a period when fetal plasma testosterone levels rise (Ward et al., 2003; Weisz and Ward, 1980) and the coiling of the epididymal portion of the WD develops (Hannema and Hughes, 2007; Welsh et al., 2006, 2007). Curiously, we observed SPAG11C localization (mRNA and protein) primarily in mesenchymal cells of the developing WD, in contrast to its predominant immunolocalization to the epithelial cells of the postnatal and adult epididymis (Ribeiro et al., 2015). As a result from the developmental and surgical castration studies, we also suggested that androgens contributed to the epididymal cell type- and region-specific modulation of SPAG11C in the developing epididymis. A potential role for this β-defensin in tissue morphogenesis was suggested due to the ubiquitous distribution of *Spag11c* mRNA in reproductive and non-reproductive organs observed in rat fetuses (Ribeiro et al., 2015). Although its physiological relevance is still unknown, the characterization of the SPAG11C spatio-temporal expression pattern in the developing rat epididymis provided the framework for the study and understanding of its function.

β-defensins are secretory small cysteine-rich cationic proteins with an alpha-helix and three beta-sheets primarily associated in adult animals with host defense through potent antimicrobial activity and immunomodulatory actions (Selsted et al., 1985; Taylor et al., 2008). In mammals they are abundantly expressed in the adult epididymal epithelial cells from where they are secreted. Their association with spermatozoa in the epididymal lumen and ejaculate have also implicated them in the regulation of sperm function and fertility (Li et al., 2001; Zhou *et al.*, 2004; Avellar *et al.*, 2007; Tollner et al., 2011; Ribeiro et al. 2012; Semple and Dorin, 2012). Indeed, a marked *in vivo* consequence of a β-defensin cluster deletion in mice was profound male sterility due to defects in sperm maturation (Zhou et al., 2013).

In view of our discovery of the spatio-temporal expression of the β-defensin SPAG11C during WD morphogenesis, we tested the hypothesis of SPAG11C as a novel androgen-target player during the regulation of WD morphogenesis. In the present work, we took advantage of an ex vivo organotypic culture of the rat WD as well as tissues from AR knockout mice (ARKO) to isolate the

85   role of testosterone/AR signaling in the regulation of the *Spag11c* gene expression (mRNA and immunolocalization) during WD differentiation. We have also tested the impact of the recombinant full-length human SPAG11C (hSPAG11C) on the ex vivo cultured WDs. The results contribute to a better understanding of the physiological relevance of the β-defensin SPAG11C during WD morphogenesis and its potential translation into the clinical setting for its suitability as a key biomarker

90   of developmental events or target for the diagnosis or treatment of diseases in the developing epididymis.

2. MATERIAL AND METHODS

2.1. Animals and tissue collection

95   Wistar rats were bred and housed in the Animal Facility at Instituto Nacional de Farmacologia/Universidade Federal de São Paulo – Escola Paulista de Medicina (UNIFESP-EPM) under controlled light (12 h light:dark cycle) and temperature (22–24 °C), with free access to food and water. To establish timed matings, a single male rat was housed overnight with two female rats. The presence of spermatozoa in vaginal smears the following morning was considered evidence of mating

100   and the time defined as embryonic day e0.5. Dams were euthanized by inhalation of an overdose of isoflurane (Cristália, Itapira, SP, Brazil) followed by bilateral pneumothorax. Fetuses were recovered, anesthetized in ice-cold DPBS (Thermo Fisher Scientific, Grand Island, NY, USA) and then decapitated. Fetal tissues were collected at e17.5 and e20.5. All procedures were conducted in compliance with the guidelines for the care and use of laboratory animal and were approved by the

105   Research Ethical Committee from UNIFESP-EPM (CEUA#1776201213).

Slides containing Bouin's-fixed paraffin-embedded tissue sections from WDs with testes attached from Androgen Receptor (AR) knockout (ARKO) and correspondent wild type (WT) mice were made available by the University of Edinburgh (UK). ARKO mice were generated by mating female mice heterozygous for the X-linked hypoxanthine phosphoribosyltransferase-Cre transgene with

110   male ARflox mice. WD/testis were collected from fetuses at e16.5 and processed for paraffin embedding as previously described (De Gendt et al., 2004; Welsh et al., 2009). E16.5 was chosen because it coincides with both the initial duct coiling in WT mice and the beginning of the duct regression in ARKO mice (Welsh et al., 2009).

115   ### 2.2. Determination of plasma testosterone concentration

Blood samples, collected following fetal decapitation, were transferred to EDTA-treated tubes

and centrifuged (1000 × g, 10 min, 4°C). Pooled plasma samples (2-3 fetuses/sample) were then aliquoted and stored at −20°C until use. Plasma testosterone concentration was measured via enzyme-linked immunosorbent assays (IBL International GMBH, Hamburg, Germany) according to manufacturer's instructions. Plates were read in a microplate spectrophotometer (Molecular Devices VERSAmax Tunable Microplate Reader, Sunnyvale, CA, USA) at 450 nm. The assay detection limit was 70 pg/ml and the detection range was 0.20–16.0 ng/ml.

2.3. Production of purified recombinant His-tagged human SPAG11C (hSPAG11C)

The DNA coding region of human SPAG11C (minus the secretory signal peptide; aminoacids M^{25}-Y^{113}; NCBI accession number NM_058203.2) was amplified by PCR. The PCR product was cloned into the expression vector pET-28a (Millipore, Darmstadt, Germany) in fusion with N-terminal 6xHis-tag and then expressed in BL21-DE3-RIL *Escherichia coli* cells after IPTG-induction (Thermo Fisher Scientific, Bleiswijk, Netherlands). The recombinant protein was purified by affinity chromatography on an Ni-NTA column (Qiagen, Valencia, CA, USA) followed by further HPLC purification on a Sep-Pack C18 cartridge (Waters, USA). Protein quality was preliminary confirmed by 4-12% SDS-PAGE analysis (Coomassie gel staining and Western Blot using antibodies anti-His and anti-SPAG11C). Then, the molecular weight of purified protein was determined by LC/ESI-MS mass spectrometry analysis and matched the theoretical mass of the hSPAG11C (13.9 kDa). Purified recombinant hSPAG11C was vacuum-dried. Lyophilized samples were aliquoted and kept at −80°C until use.

2.4. WD organotypic culture

The organotypic culture of WDs, that mimics the in vivo androgen-dependent WD morphological differentiation, was performed as described by Tsuji et al. (1991) with modifications. In

brief, the whole urogenital tract was dissected from male rat fetuses at e17.5 in ice-cold DPBS (Thermo Fisher Scientific) under a Stemi 2000C stereomicroscope (Carl Zeiss MicroImaging GmbH, Jena, Germany). Isolated WDs without testis, but including the prospective efferent ducts and the vas deferens, were placed on a 30 mm Millicell hydrophilic polytetrafluoroethylene inserts (Merck Millipore, Tullagreen, Carrigtwohill, Ireland). The inserts, each containing two-three WDs, were then transferred to individual wells of 6-well plates floating on 1.5 ml of serum-free medium composed of DMEM/F12 (Thermo Fisher Scientific, Grand Island, NY, USA), 1% insulin−transferrin−selenium (Thermo Fisher Scientific) and 50 μg/mL ampicillin (Sigma-Aldrich, Bornem, Belgium) and supplemented with testosterone (0.1-10 nM; Sigma-Aldrich, St. Louis, MO, USA). Cultures were kept in a humidified incubator at 37°C with a 5% CO_2/95% air for up to 96 h. Changes of fresh medium were performed every 24 h, unless otherwise mentioned. Gross morphology of cultured WDs was inspected using a Nikon Ti-U inverted microscope (Nikon Instruments Inc, Melville, NY, USA). Whole-mount images were acquired immediately after WDs were placed into culture (0 h) and then daily until culture was terminated. At the end of the culture, WDs were processed for reverse transcription followed by real-time quantitative PCR studies (RT-qPCR) or immunofluorescence assays.

2.5. Androgen-dependency studies using WD organotypic culture

Isolated e17.5 WDs were cultured for up to 96 h with fresh medium supplemented with increasing concentrations of testosterone (0.1-10 nM). Ducts were also cultured in the absence or presence of flutamide (10 μM; Sigma-Aldrich, St. Louis, MO, USA), a nonsteroidal AR competitive antagonist (Ki ≅ 3.40 μM; Simard et al., 1986), as well as in the presence of testosterone (10 nM) and flutamide (10 μM). An equivalent volume of ethanol (diluent of testosterone) was added to the culture medium and used as a control. Gross morphology was inspected as described before. At specific time-

8

165 points, tissues were collected and used for RT-qPCR and immunofluorescence studies.

2.6. Evaluation of hSPAG11C-induced effects on morphogenesis of cultured WDs

Isolated e17.5 WDs were cultured for up to 96 h in medium supplemented with purified recombinant hSPAG11C (80 nM) or equivalent molar concentration of bovine serum albumin (BSA) used as unspecific protein control. This hSPAG11C working concentration was selected based on

170 preliminary mammalian cell culture experiments in which the concentration range of 0.8–800 nM of this recombinant protein was not toxic to the cells (data not shown). The specificity of the hSPAG11C-induced effects was evaluated by washout experiments, in which hSPAG11C was removed after 48 h of its incubation and WDs then allowed to develop for 48 h more in fresh medium. Gross morphology was inspected as previously described above. Immunofluorescence assays using anti-His antibody were

175 performed to check the ability of purified recombinant hSPAG11C to be taken up by the cultured WD cells.

2.7. Measurement of WD elongation and coiling

WD morphological differentiation ex vivo was quantified by measuring the length and the

180 number of bends along the portion of the duct that will become the future epididymis, i.e., from the end of the merging efferent ducts to the intersection between cauda epididymis and vas deferens wherein a symmetric U-shape is found. Quantifications were performed on whole-mount images using the ImageJ software (Schindelin et al., 2012). Firstly, when necessary, two images taken at low magnification were stitched together using the Pairwise Stitching plugin (Preibisch et al., 2009). The

185 digital images were then spatially calibrated and a freehand line was drawn along the duct and the length distance was measured (mm). WD coiling was quantified by measuring the number of bends along the duct. Two intersecting lines were drawn outlining WD lumen and then the central angle of each curve was measured using the angle tool. One bend was defined by a central angle narrow than

60° as previously described (Xu et al., 2016).

190   *2.8. Real-time quantitative PCR (qPCR)*

Total RNA was extracted from frozen isolated WDs by using Pico Pure RNA isolation kit (Thermo Fisher Scientific, Foster City, CA, USA). Total RNA quantity and quality (absorbance ratios A260:A280 and A260:A230 > 1.8) were assessed with a NanoVue spectrophotometer (GE Healthcare Life Sciences, Fairfield, CT, USA) and 1 μg was used in reverse transcriptase reactions containing

195   oligo(dT) following the manufacture's instructions (Thermoscript RT-PCR system; Thermo Fisher Scientific, CA, USA).

cDNA samples were assayed in qPCR performed with SYBR Green Master Kit (Kapa Biosystems, Cape Town, South Africa) in an ABI PRISM 7500 Sequence Detection System (Applied Biosystems, Foster City, CA, USA) using primers targeting rat *Spag11c* and *Acta2* genes, as previously

200   described (Ribeiro et al., 2015). The mRNA levels of *Acta2*, which is a specific marker for peritubular smooth muscle cells known to be up-regulated during WD development (Hannema et al., 2006; Welsh et al., 2006; Ribeiro et al., 2015), was used as a positive control. At the end of each reaction, a melting curve was generated and analyzed to confirm the specificity of the amplified PCR product. The average cycle threshold (Ct) was automatically determined using the 7500 Applied Biosystems software

205   (version 2.0.5). Relative quantification of target genes was calculated using the method $2^{-\Delta\Delta Ct}$ (Livak and Schmittgen, 2001). *Rpl19 (Ribosomal protein L19*) housekeeping gene, which was stably expressed among samples, was used for the internal standardization of the qPCR results (*Rpl19* Ct variation values: standard deviation ≤ 0.45 and coefficient of variation ≤ 2.30%, n=21-25 samples).

210   *2.9. Immunofluorescence*

Isolated WDs were fixed in 4% paraformaldehyde in PBS for 2 h at 4°C, dehydrated through a sucrose gradient (10-30%) and then embedded using freezing media as previously described (Liu et al.,

10

2012). Immunofluorescence localization of proteins using cryosections (8-10 μm) was performed as previously described (Queiróz et al., 2008). In brief, tissue sections were washed in PBS and incubated

215   for 1 h at room temperature with blocking solution composed of PBS 0.1 M (pH 7.4), 3% albumin (w/v) and 0.01% saponin, (w/v). Sections were then incubated for 16 h at 4°C in blocking solution containing the following primary antibodies, all polyclonal and produced in rabbit: antibody anti-SPAG11C (Imuny, Campinas, SP, Brazil; cat. IPVS-1023; antigen sequence: METQVGYCSKKKEA; 1:200 v/v working dilution based on Ribeiro et al., 2015), antibody anti-alpha smooth muscle actin

220   (Abcam, cat. ab5694, 1:50 v/v working dilution), antibody anti-androgen receptor (Santa Cruz, cat. sc-816, 1:200 v/v working dilution), antibody anti-phospho-histone-H3 (Millipore, cat. 06-570, 1:200 v/v working dilution) and antibody anti-cleaved caspase-3 (Cell Signaling, cat. sc- 9661S, 1:200 v/v working dilution). Monoclonal anti-polyhistidine antibody produced in mice was also used (Sigma, cat. H1029, 1:3000 v/v working dilution). After washes in PBS, sections were incubated for 1 h at room

225   temperature in blocking solution with either donkey anti-rabbit or goat anti-mouse secondary antibody conjugated to Alexa Fluor 594 (Molecular Probes, 1:200 v/v working dilution). DAPI (4,6-diamidino-2-phenylindole) was used for nuclear identification. Slides were coverslipped with ProLong Gold (Molecular Probes). Negative controls were performed by either replacing the primary antibody with nonimmune rabbit serum or by pre-adsorption of the primary antibody with 10-fold molar excess of its

230   corresponding antigen peptide. Images were obtained with identical settings on the Leica TCS SP8 inverted confocal microscope (Leica Microsystems, Wetzlar, Germany) unless otherwise specified. Representative images of each group were selected.

2.10. Measurement of cell proliferation and apoptosis

235   Immunofluorescence studies for phospho-histone H3 (pH3, mitotic cell immunomarker) and cleaved caspase-3 (apoptotic cell immunomarker) were performed in cryosections of WDs cultured in

absence and presence of recombinant hSPAG11C. Measurement of the number of epithelial proliferative cells was based on the procedure described by Welsh et al. (2006). The whole epididymal portion of each WD was visualized in one microscope field using a 20x objective (Nikon E800; Nikon, Melville, NY, USA). The digital images were captured using a Retiga 2000R CCD camera (QImaging, Surrey, Canada) and then imported into Image J software, where the number of pH3-positive WD epithelial cells were manually counted using the Cell Counter Image J plugin. The total number of pH3-positive cells was then normalized against the total surface of the epithelium length/microscope field that was also measured using ImageJ software. This parameter, which corresponded to the sum of the perimeter of multiple surfaces of a single tubule in each tissue cryosection analyzed, was used as a correction factor for differences per slide in the plane of the tissue sectioning and/or effect of culture treatment. The number of proliferating cells was expressed in terms of pH3-positive cells/mm of WD epithelium. At least 6-7 microscope fields of WDs from a total of 4 fetuses per experimental group were evaluated. To assess the precision of the cell counting, all sections were counted independently by at least two trained observers.

2.11. Statistical analysis

Values were expressed as mean ± SEM. For two group comparisons, two-tailed Student's t-test was applied. For multiple group comparisons, one-way ANOVA was performed. GraphPad Prism software version 5 (Graph Pad Software) was used for all statistical analysis. $P < 0.05$ was considered statistically significant.

3. RESULTS

3.1. Influence of androgens on Spag11c mRNA levels in WD organotypic culture

260   First, we independently confirmed that the three-fold decrease in the *Spag11c* mRNA levels in the developing WDs between e17.5 (uncoiled duct) and e20.5 (coiled duct) observed in our previous study (Ribeiro et al., 2015) occurred in parallel with a significant increase in the plasma testosterone concentrations in these male fetuses (4.63 ± 0.45 nM at e17.5 versus 7.73 ± 0.55 nM at e20.5; mean $\pm$ SEM; n=7 pools/age; t test, *p<0.05).

265   Next we used the ex vivo WD organotypic culture to check if the in vivo *Spag11c* mRNA changes in the developing WDs cited above could be directly attributed to the effects of testosterone/AR signaling on this gene expression in the duct. Temporal morphological changes were observed when e17.5 WDs were cultured for up to 72 h in the absence (Fig. 1A-C, Fig. 2A-D) or presence of increasing concentrations of testosterone (Fig. 1 D-L). As expected, WD elongation and

270   coiling were prevented when ducts were exposure to both testosterone and flutamide (Fig. 2 M-P).

       A significant reduction in the *Spag11c* transcript levels was observed in WDs cultured for 72 h in the presence of 10 nM testosterone (Fig. 1M). The *Spag11c* mRNA downregulation was observed as early as 24 h after culture, when no dramatic gross morphological changes such as observed after 72 h of incubation, had taken place (Fig. 2). This observation suggests that mRNA changes were not simply

275   a consequence of changes in cellular type composition during WD development. Furthermore, the testosterone-induced down-regulation of *Spag11c* mRNA levels was, at least partially, reduced by co-incubation of testosterone (10 nM) with flutamide (10 μM) (Fig. 2Q), suggesting the androgen responsiveness of these parameters. Conversely, in spite of the expected testosterone-induced increase in *Acta2* mRNA levels and its abrogation by flutamide in WDs cultured for 72 h (Fig. 1M, Fig. 2Q), a

280   downregulation of *Acta2* transcript levels was observed when ducts were exposed to testosterone for 24 h (Fig. 2Q).

3.2. Influence of androgens on Spag11c immunolocalization in WD organotypic culture

Immunoflurescence studies confirmed the predominant localization of SPAG11C in the mesenchymal cells from isolated WDs at ages e17.5 and e20.5 (Fig. 3A-C). This expression pattern was also observed when e17.5 WDs were cultured ex vivo with testosterone (10 nM) for either 48 h (Fig. 3H) or 72 h (Fig. 3J). Under testosterone-deprived culture condition, SPAG11C immunoreactivity in stromal cells was still present after 48 h (Fig. 3G), while it decreased significantly with progression of the culture to 72 h (Fig. 3I). Ducts kept in culture after 72 h with both testosterone (10 nM) and flutamide (10 μM) also presented a significant decrease in SPAG11C immunofluorescence (Fig. S1), confirming the androgen effects on SPAG11C expression at the protein level.

ACTA2 immunoreactivity was observed in stromal cells directly surrounding the WD from e17.5 and e20.5 male fetuses (Fig. 3D-F). The immunodistribution pattern of this smooth muscle specific marker, however, was not significantly influenced by the androgenic conditions of WDs in culture (Fig. 3K-N).

3.3. SPAG11C immunolocalization in the WD from ARKO mice

To gain insight into the in vivo regulation of SPAG11C in the developing WD by testosterone/AR signaling, we next performed immunofluorescence studies in tissue sections from the ARKO fetuses mice. The SPAG11C distribution pattern observed in WD from WT mice (Figs. 4A-G) was similar to that previously described in age-matched Wistar rats (Ribeiro et al., 2015). SPAG11C immunoreactivity in control WDs was restricted to the mesenchymal compartment, with the strongest fluorescent signal being detected in stromal cells that do not directly surround the duct epithelium (Figs. 4A-G). The lack of AR signaling resulted in changes in SPAG11C immunoreactivity pattern with higher fluorescent intensity observed in periductal stromal cells from ARKO WDs when compared to the WT tissues (Figs. 4H-N). In addition, ACTA2 immunoreactivity was maintained in

14

the WD stromal cells of ARKO tissues (Figs. 4O-Q).

3.4. Effects of recombinant hSPAG11C on WD morphogenesis ex vivo

To determine a functional response of the β-defensin SPAG11C on WD morphogenesis, we

310   evaluated the effects of the recombinant protein hSPAG11C on the WD morphogenesis *ex vivo*.

hSPAG11C-treated WDs were shorter in length and less coiled than the control ducts incubated with

BSA (Fig. 5A-F). WD coiling was partially rescued following washout of hSPAG11C and change to

normal culture medium, showing the specificity of the recombinant protein-induced effects (Fig. 5G-I).

Both the duct length and the bend numbers were reduced in WDs incubated with hSPAG11C (Fig. 5J-

315   K). These same ducts presented approximately two-fold reduction in the number of proliferating

epithelial cells (Fig. 5L-N). In addition, only rare apoptotic cells were detected in both control and

hSPAG11C-treated WDs (Fig. S2). Anti-His immunofluorescence was detected in both epithelial and

mesenchymal cells of hSPAG11C-treated WDs, demonstrating their ability to take up this recombinant

protein (Figs. 5O-Q).

320

4. DISCUSSION

The WD undergoes morphological changes over time to originate an epididymis of proper shape and length, which is critical to providing a suitable environment for sperm maturation. This highly coordinated morphogenic program is primarily orchestrated by androgens and depends upon a

325   crosstalk between WD mesenchymal and epithelial cells. The complex signaling network involving molecules of mesenchymal origin which instruct epithelial growth under control of androgen action, however, is still poorly understood (Murashima et al., 2015b). The localization of the β-defensin SPAG11C in WD mesenchymal cells and its regulation during epididymal development (Ribeiro et al., 2015) raised the possibility that this particular protein is required for WD morphogenesis. Herein, we

330   demonstrated that AR signaling drives SPAG11C expression during WD morphogenesis. Furthermore, we showed that recombinant hSPAG11C protein interfered with WD morphogenesis ex vivo by regulating epithelial cell proliferation. This implied a role for SPAG11C in the androgen-induced morphological differentiation of WD.

Our data using the rat WD organotypic culture show *Spag11c* gene as an androgen-dependent

335   target that is differentially regulated at mRNA and protein levels during the duct development. Discrepancy in the regulation of *Acta2* expression at mRNA and protein level by androgens was likewise observed. In vitro, testosterone decreased *Spag11c* mRNA levels while maintaining SPAG11C immunoreactivity in WD mesenchymal cells. Possible explanations for the apparent lack of correlation between mRNA and protein levels can be attributed to androgen-regulated post-

340   transcriptional mechanisms that can influence *Spag11c* mRNA half-life and its polysome-bound fraction, as well as protein half-life and translation rate. The clarification of these regulatory mechanisms will need further confirmation.

The relevance of androgen/AR signaling in the regulation of SPAG11C in the developing WD was further tested in a whole-system model, the ARKO mice, where AR signaling is impaired. In these

16

345   mice, changes in SPAG11C cellular distribution in the stromal compartment were observed as early as

e16.5. Based on WD coiling temporal changes, this e16.5 age-point in mice corresponds to e19.5 in

rats (Welsh et al., 2009; Hinton et al., 2011), which in turn would be comparable to e17.5 rat WDs

cultured for 48 h (i.e., 17.5 + 2 days) in the presence of testosterone.

In light of the time-dependent reduction of SPAG11C immunoreactivity observed in e17.5 rat

350   WDs cultured under androgen-deprived conditions, we could predict that SPAG11C

immunofluorescence in ARKO mice would not be maintained at age points later than e16.5. Thus, it

will be instructive to expand the analysis of SPAG11C cellular distribution in tissues from ARKO mice

at age points later than e16.5. Furthermore, the ablation of androgen signaling can disrupt the paracrine

signaling between mesenchyme and epithelium (Welsh et al., 2006, 2007) and it is suggested that

355   changes in SPAG11C immunolocalization, as a consequence, contributes to duct regression.

Conversely, no change in ACTA2 immunodistribution pattern was observed either when rat WDs were

cultured in the absence of testosterone or in ARKO tissues. These results agree with the finding that the

initiation of ACTA2 protein expression, but not its maintenance, in testicular peritubular cells is

dependent on androgens (Schlatt et al., 1993).

360   The androgen responsiveness of the *Spag11c* gene at the transcriptional level is consistent with

the identification of putative binding sites for AR in the proximal 1,000 bp of the human SPAG11B

gene promoter region that drives transcription of the *SPAG11C* mRNA splicing variant. Four 5'-

TGTTCT-3' (or 5'-AGAACA-3') sites that correspond to one-half of the near-palindromic consensus

sequence of the androgen response element (ARE) were found (Fröhlich et al., 2001). Furthermore,

365   studies using in vivo models have extensively shown androgens as important regulators of β-defensin

expression in postnatal and adult epididymis (Hamil et al., 2000; Ibrahim et al., 2001; Liu et al., 2001;

Palladino et al., 2003; Avellar et al 2004, 2007; Jalkanen et al, 2005; Radhakrishnan et al, 2005;

Yenugu et al., 2006ab; Zhao et al., 2011; Pujianto et al., 2013; Ribeiro et al., 2015). The understanding

of the molecular mechanisms by which *Spag11c* and other β-defensin genes are regulated by androgens

370 remains to be further explored.

It is worth noting that *Spag11c* mRNA was detected in the urogenital rudiment at e12.5 (Ribeiro et al., 2016), thus prior to testosterone synthesis and AR expression in rat fetuses. Moreover, *Spag11c* detection in the paramesonephric duct of female embryos demonstrates that *Spag11c* gene expression is not male-specific (Fig. S3). Following the developmental expression pattern of many

375 other morphogens such as *Inhba* (Tomaszewski et al., 2007), the results suggest the co-participation of yet-to-be-discovered androgen-independent components in the regulation of SPAG11C in the developing WD as well.

To gain insights into the SPAG11C functionality in WD morphogenesis, we analyzed the developmental pattern of WDs incubated with purified recombinant protein hSPAG11C. hSPAG11C

380 incubation reduced duct elongation and coiling as a result of significant decrease in epithelial cell proliferation, and not changes in apoptosis. This effect on the epithelium, in addition to the secretory nature of β-defensins, as well as the SPAG11C androgen-dependence and predominant localization in mesenchymal cells provide evidence to support the hypothesis that SPAG11C acts as an androgen target of mesenchymal origin regulating duct morphogenesis. Therefore, our findings provide evidence

385 that this β-defensin is a suppressor signal that opposes the ductal epithelial cell proliferation induced by testosterone. The dynamic modulation of SPAG11C expression at mRNA and protein levels by testosterone would thus contribute to the delicate balance between anti- and pro-proliferative signals that allow proper WD elongation and coiling.

β-defensins, are multifunctional proteins that can affect diverse cellular processes (*i.e.*, cell

390 proliferation, differentiation and migration) and are known to display opposing functions depending upon their concentrations and targeted cell types (for review, see Semple and Dorin, 2012). Likewise SPAG11C, several human β-defensins (e.g. hBD1, hBD2, hBD3, and hBD4) act as proliferation-

repressor signals at nanomolar concentration (Pingel et al., 2008; Winter et al., 2011; Zhuravel et al., 2011; Gerashchenko et al., 2014). Cell cycle arrest at G1 phase (Zhuravel et al., 2011) and inhibition of ERK phosphorylation (Pingel et al., 2008) are also proposed mechanisms by which β-defensins can suppress cell proliferation.

We recently reported that in contrast to *Spag11c* mRNA detection in WDs at both e17.5 and e20.5, transcripts for *Defb1*, *Defb2* and *Defb22* were primarily observed in e20.5 WDs, while *Defb12* and *Spag11e* mRNAs were not readily detected at these two age points (Ribeiro et al., 2016). This unique expression pattern of *Spag11c* mRNA in WD in comparison to other β-defensins suggests functional specialization of the members of this protein family during WD morphogenesis. Moreover, β-defensins may differentially respond to developmental cues, which further suggests diverse mechanisms by which their expression is regulated. Our future experiments will be directed towards examining the physiological role(s) and mechanism(s) of action of SPAG11C in vivo.

In summary, our data suggest that androgen/AR signaling modulates SPAG11C expression and regulates WD epithelial proliferation. These findings highlight the putative relevance of homeostatic patterns of in utero expression of SPAG11C and presumably of other β-defensins for proper masculinization of the male reproductive tract.

5. AUTHOR CONTRIBUTIONS

CMR, BTH and MCWA designed research, analyzed data and wrote the paper. CMR, LGAF, DST performed research and analyzed data. LBS contributed materials and help with research design and analyses.

6. ACKNOWLEDGMENTS

7. REFERENCES

430   Archambeault DR, Tomaszewski J, Joseph A, Hinton BT, Yao HH. Epithelial-mesenchymal crosstalk in Wolffian duct and fetal testis cord development. *Genesis*, 47:40-8, 2009.

Avellar MC, Honda L, Hamil KG, Yenugu S, Grossman G, Petrusz P, French FS, Hall SH. Differential expression and antibacterial activity of epididymis protein 2 isoforms in the male reproductive tract of human and rhesus monkey (Macaca mulatta). *Biol Reprod*, v.71, p.1453-60, 2004.

435   Avellar MC, Honda L, Hamil KG, Radhakrishnan Y, Yenugu S, Grossman G, Petrusz P, French FS, Hall SH. Novel aspects of the sperm-associated antigen 11 (SPAG11) gene organization and expression in cattle (Bos taurus). *Biol Reprod*, v. 76, n. 6, p.1103-16, 2007.

Björkgren I, Alvarez L, Blank N, Balbach M, Turunen H, Laajala TD, Toivanen J, Krutskikh A, Wahlberg N, Huhtaniemi I, Poutanen M, Wachten D, Sipilä P. Targeted inactivation of the mouse
440   epididymal beta-defensin 41 alters sperm flagellar beat pattern and zona pellucida binding. *Mol Cell Endocrinol*, v.427, p.143-54, 2016.

Carroll TJ, Park JS, Hayashi S, Majumdar A, McMahon AP. Wnt9b plays a central role in the regulation of mesenchymal to epithelial transitions underlying organogenesis of the mammalian urogenital system. *Dev Cell*, v.9, n.2, p.283-92, 2005.

445   De Gendt K, Swinnen JV, Saunders PT, Schoonjans L, Dewerchin M, Devos A, Tan K, Atanassova N, Claessens F, Le ́cureuil C, Heyns W, Carmeliet P, Guillou F, Sharpe RM, Verhoeven G. A Sertoli cell-selective knockout of the androgen receptor causes spermatogenic arrest in meiosis. *Proc Natl Acad Sci USA*, v.101, p.1327–32, 2004.

Diao R, Fok KL, Chen H, Yu MK, Duan Y, Chung CM, Li Z, Wu H, Li Z, Zhang H, Ji Z, Zhen W, Ng
450   CF, Gui Y, Cai Z, Chan HC. Deficient human β-defensin 1 underlies male infertility associated with poor sperm motility and genital tract infection. *Sci Transl Med*, v. 6: 249ra108, 2014.

Dorin JR, Barratt CL. Importance of β-defensins in sperm function. *Mol Hum Reprod*, v. 20, n. 9,

p.821-6, 2014.

Fröhlich O, Po C, Young LG. Organization of the human gene encoding the epididymis-specific EP2
455   protein variants and its relationship to defensin genes. *Biol Reprod*, v.64, p.1072-79, 2001.

Gerashchenko O, Zhuravel E, Skachkova O, Khranovska N, Pushkarev V, Pogrebnoy P, Soldatkina M.
Involvement of human beta-defensin-2 in regulation of malignant potential of cultured human
melanoma cells. *Exp Oncol*, v.36, n.1, p.17-23, 2014.

Gupta C. The role of epidermal growth factor receptor (EGFR) in male reproductive tract
460   differentiation: stimulation of EGFR expression and inhibition of Wolffian duct differentiation with
anti-EGFR antibody. *Endocrinology*, v.137, n.3, p.905-10, 1996.

Hamil KG, Sivashanmugam P, Richardson RT, Grossman G, Ruben SM, Mohler JL, Petrusz P, O'Rand
MG, French FS, Hall S.H. HE2beta and HE2gamma, new members of an epididymis-specific family
of androgen-regulated proteins in the human. *Endocrinology*, v.141, n. 3, p. 1245-53, 2000.

465   Hannema SE, Hughes IA. Regulation of Wolffian duct development. *Horm Res*, v.67, n.3, p. 142-51,
2007.

Hannema SE, Print CG, Charnock-Jones DS, Coleman N, Hughes IA. Changes in gene expression
during Wolffian duct development. *Horm Res*, v.65, n.4, p.200-9, 2006.

Hinton BT, Galdamez MM, Sutherland A, Bomgardner D, Xu B, Abdel-Fattah R, Yang, L. How do
470   you get six meters of epididymis inside a human scrotum? *J Androl*, v.32, n.6, p.558-64, 2011.

Ibrahim NM, Young LG, Fröhlich O. Epididymal specificity and androgen Regulation of rat EP2. *Biol
Reprod*, v.65, n.2, p.575-80, 2001.

Imperato-McGinley J, Sanchez RS, Spencer JR, Yee B, Vaughan ED. Comparison of the effects of the
5 alpha-reductase inhibitor finasteride and the antiandrogen flutamide on prostate and genital
475   differentiation: dose-response studies. *Endocrinology*, v.131, n.3, p.1149-56, 1992.

Jalkanen J, Huhtaniemi I, Poutanen M. Discovery and characterization of new epididymis-specific

beta-defensins in mice. *Biochim Biophys Acta*, v.1730, n.1, p.22-30, 2005.

Kitagaki J, Ueda Y, Chi X, Sharma N, Elder CM, Truffer E, Costantini F, Lewandoski M, Perantoni AO. FGF8 is essential for formation of the ductal system in the male reproductive tract. *Development*, v.138, n.24, p.5369-78, 2011.

Kumar M, Syed SM, Taketo MM, Tanwar PS. Epithelial Wnt/β-catenin signalling is essential for epididymal coiling. *Dev Biol*, v.412, n.2, p.234-49, 2016.

Li P, Chan HC, He B, So SC, Chung YW, Shang Q, Zhang YD, Zhang YL. An antimicrobial peptide gene found in the male reproductive system of rats. *Science*, v.291, n.5509, p.1783-5, 2001.

Liu C, Paczkowski M, Othman M, Yao HH. Investigating the origins of somatic cell populations in the perinatal mouse ovaries using genetic lineage tracing and immunohistochemistry. *Methods Mol Biol*, v.825, p.211-21, 2012.

Liu Q, Hamil KG, Sivashanmugam P, Grossman G, Soundararajan R, Rao AJ, Richardson RT, Zhang YL, O'Rand MG, Petrusz P, French FS, Hall SH. Primate epididymis-specific proteins: characterization of ESC42, a novel protein containing a trefoil-like motif in monkey and human. *Endocrinology*, v.142, n.10, p.4529-39, 2001.

Livak KJ, Schmittgen TD. Analysis of relative gene expression data using real-time quantitative PCR and the 2(-Delta Delta C(T)) Method. *Methods*, v.25, n.4, p.402-8, 2001.

Murashima A, Miyagawa S, Ogino Y, Nishida-Fukuda H, Araki K, Matsumoto T, Kaneko T, Yoshinaga K, Yamamura K, Kurita T, Kato S, Moon AM, Yamada G. Essential roles of androgen signaling in Wolffian duct stabilization and epididymal cell differentiation. *Endocrinology*, v.152, n.4, p.1640-51, 2011.

Murashima A, Kishigami S, Thomson A, Yamada G. Androgens and mammalian male reproductive tract development. *Biochim Biophys Acta*, v.1849, n.2, p.163-70, 2015a.

Murashima A, Xu B, Hinton BT. Understanding normal and abnormal development of the

Wolffian/epididymal duct by using transgenic mice. *Asian J Androl*, v.17, n.5, p.749-55, 2015b.

Okazawa M, Murashima A, Harada M, Nakagata N, Noguchi M, Morimoto M, Kimura T, Ornitz DM, Yamada G. Region-specific regulation of cell proliferation by FGF receptor signaling during the Wolffian duct development. *Dev Biol*, v.400, n.1, p.139-47, 2015.

505   Palladino MA, Mallonga TA, Mishra MS. Messenger RNA (mRNA) expression for the antimicrobial peptides β-defensin-1 and β-defensin-2 in the male rat reproductive tract: β-defensin-1 mRNA in initial segment and caput epididymidis is regulated by androgens and not bacterial lipopolysaccharides. *Biol Reprod*, v.68, n.2, p.509-515, 2003.

Pingel LC, Kohlgraf KG, Hansen CJ, Eastman CG, Dietrich DE, Burnell KK, Srikantha RN, Xiao X,

510   Bélanger M, Progulske-Fox A, Cavanaugh JE, Guthmiller JM, Johnson GK, Joly S, Kurago ZB, Dawson DV, Brogden KA. Human β-defensin 3 binds to hemagglutinin B (rHagB), a non-fimbrial adhesin from Porphyromonas gingivalis, and attenuates a pro-inflammatory cytokine response. *Immunol Cell Biol*, v.86, n.8, p.643-9, 2008.

Preibisch S, Saalfeld S, Tomancak P. Globally optimal stitching of tiled 3D microscopic image

515   acquisitions, *Bioinformatics*, v.25, n.11, p.1463-65, 2009.

Pujianto DA, Loanda E, Sari P, Midoen YH, Soeharso P. Sperm-associated antigen 11A is expressed exclusively in the principal cells of the mouse caput epididymis in an androgen-dependent manner. *Reprod Biol Endocrinol*, v.11, p.1-12, 2013.

Queiróz DB, Porto CS, Grossman G, Petrusz P, Avellar MC. Immunolocalization of alpha(1A)-

520   adrenoceptors in rat and human epididymis. *Cell Tissue Res*, v. 332, n. 3, p. 509-22, 2008.

Radhakrishnan Y, Hamil KG, Yenugu S, Young SL, French FS, Hall SH. Identification, characterization, and evolution of a primate β-defensin gene cluster. *Genes Immun*, v.6, p.203-210, 2005.

Ribeiro CM, Romano RM, Avellar MCW. β-defensins in the epididymis: clues to multifunctional

525   roles. *Anim Reprod*, v.9, n.4, p.751-759, 2012.

Ribeiro CM, Queiróz DB, Patrão MT, Denadai-Souza A, Romano RM, Silva EJ, Avellar MC. Dynamic changes in the spatio-temporal expression of the β-defensin SPAG11C in the developing rat epididymis and its regulation by androgens. *Mol Cell Endocrinol*, v.404, p.141-50, 2015.

Ribeiro CM, Silva EJ, Hinton BT, Avellar MC. β-defensins and the epididymis: contrasting influences

530   of prenatal, postnatal, and adult scenarios. *Asian J Androl*, v.18, n.2, p.323-28, 2016.

Selsted ME, Harwig SS, Ganz T, Schilling JW, Lehrer RI. Primary structures of three human neutrophil defensins. *J Clin Invest*, v.76, n.4, p.1436-9, 1985.

Semple F, Dorin JR. β-Defensins: multifunctional modulators of infection, inflammation and more?. *J Innate Immun*, v.4, n.4, p.337-48, 2012.

535   Schlatt S, Weinbauer GF, Arslan M, Nieschlag E. Appearance of alpha-smooth muscle actin in peritubular cells of monkey testes is induced by androgens, modulated by follicle-stimulating hormone, and maintained after hormonal withdrawal. *J Androl*, v. 14, n.5, p.340-50, 1993.

Schindelin J, Arganda-Carreras I, Frise E, Kaynig V, Longair M, Pietzsch T, Preibisch S, Rueden C, Saalfeld S, Schmid B, Tinevez JY, White DJ, Hartenstein V, Eliceiri K, Tomancak P, Cardona A.

540   Fiji: an open-source platform for biological-image analysis. *Nat Methods*, v.9, n.7, p.676-82, 2012.

Simard J, Luthy I, Guay J, Bélanger A, Labrie F. Characteristics of interaction of the antiandrogen flutamide with the androgen receptor in various target tissues. *Mol Cell Endocrinol*, v.44, n.3, p.261-70, 1986.

Taylor K, Barran PE, Dorin JR. Structure-activity relationships in β-defensin peptides. *Biopolymers*,

545   v.90, n.1, p.1-7, 2008.

Tollner TL, Venners SA, Hollox EJ, Yudin AI, Liu X, Tang G, Xing H, Kays RJ, Lau T, Overstreet JW, Xu X, Bevins CL, Cherr GN. A common mutation in the defensin DEFB126 causes impaired sperm function and subfertility. *Sci Transl Med*, v.3, n.92, p.ra65, 2011.

Tomaszewski J, Joseph A, Archambeault D, Yao HH. Essential roles of inhibin beta A in mouse

550   epididymal coiling. *Proc Natl Acad Sci U S A*, v.104, n.27, p.11322-7, 2007.

Tsuji M, Shima H, Cunha GR. In vitro androgen-induced growth and morphogenesis of the Wolffian

duct within urogenital ridge. *Endocrinology*, v.128, n.4, p. 805-11, 1991.

Xu B, Washington AM, Domeniconi RF, Ferreira Souza AC, Lu X, Sutherland A, Hinton BT. Protein

tyrosine kinase 7 is essential for tubular morphogenesis of the Wolffian duct. *Dev Biol*, v.412, n.2,

555   p.219-33, 2016.

Ward IL, Ward OB, Affuso JD, Long WD 3rd, French JA, Hendricks SE Fetal testosterone surge:

specific modulations induced in male rats by maternal stress and/or alcohol consumption. *Horm
Behav*, v.43, n.5, p.531-9, 2003.

Weisz J, Ward IL. Plasma testosterone and progesterone titers of pregnant rats, their male and female

560   fetuses, and neonatal offspring. *Endocrinology*, v.106, n.1, p.306-16, 1980.

Welsh M, Saunders PT, Marchetti NI, Sharpe, RM. Androgen-dependent mechanisms of Wolffian duct

development and their perturbation by flutamide. *Endocrinology*, v.147, n.10, p.4820-30, 2006.

Welsh M, Saunders PT, Sharpe R.M. The critical time window for androgen-dependent development

of the Wolffian duct in the rat. *Endocrinology*, v.148, n.7, p.3185-95, 2007.

565   Welsh M, Saunders PT, Fisken M, Scott HM, Hutchison GR, Smith LB, Sharpe RM. Identification in

rats of a programming window for reproductive tract masculinization, disruption of which leads to

hypospadias and cryptorchidism. *J Clin Invest*, v.118, n.4, p.1479-90, 2008.

Welsh M, Sharpe RM, Walker M, Smith LB, Saunders PT. New insights into the role of androgens in

Wolffian duct stabilization in male and female rodents. *Endocrinology*, v.150, n.5, p.2472-80, 2009.

570   Winter J, Pantelis A, Reich R, Martini M, Kraus D, Jepsen S, Allam JP, Novak N, Wenghoefer M.

Human β-defensin-1, -2, and -3 exhibit opposite effects on oral squamous cell carcinoma cell

proliferation. *Cancer Invest*, v.29, n.3, p.196-201, 2011.

Yenugu S, Chintalgattu V, Wingard CJ, Radhakrishnan Y, French FS, Hall SH. Identification, cloning

and functional characterization of novel β-defensins in the rat (Rattus norvegicus). *Reprod Biol*

575   *Endocrinol*, v.4, p.7, 2006a.

Yenugu S, Hamil KG, Grossman G, Petrusz P, French FS, Hall SH. Identification, cloning and functional characterization of novel sperm associated antigen 11 (SPAG11) isoforms in the rat. *Reprod Biol Endocrinol*, v.4, n.23, 2006b.

Zhao Y, Diao H, Ni Z, Hu S, Yu H, Zhang Y. The epididymis-specific antimicrobial peptide β-defensin

580   15 is required for sperm motility and male fertility in the rat (Rattus norvegicus). *Cell Mol Life Sci*, v.68, p.697-708, 2011.

Zhou CX, Zhang YL, Xiao L, Zheng M, Leung KM, Chan MY, Lo PS, Tsang LL, Wong HY, Ho LS, Chung YW, Chan HC. An epididymis-specific β-defensin is important for the initiation of sperm maturation. *Nat Cell Biol*, v. 6, n. 5, p. 458-64, 2004.

585   Zhou YS, Webb S, Lettice L, Tardif S, Kilanowski F, Tyrrell C, Macpherson H, Semple F, Tennant P, Baker T, Hart A, Devenney P, Perry P, Davey T, Barran P, Barratt CL, Dorin JR. Partial Deletion of Chromosome 8 β-defensin Cluster Confers Sperm Dysfunction and Infertility in Male Mice. *PLoS Genet*, v.9, n.10, p.e1003826, 2013.

Zhuravel E, Shestakova T, Efanova O, Yusefovich Y, Lytvin D, Soldatkina M, Pogrebnoy P. Human β-

590   defensin-2 controls cell cycle in malignant epithelial cells: in vitro study. *Exp Oncol*, v.33, n.3, p.114-20, 2011.

595 **Fig. 1. Morphological differentiation and mRNA expression pattern of rat Wolffian duct (WD) cultured with increasing testosterone concentrations.** Morphological changes (A-L) and mRNA levels (M) of WDs collected at e17.5 and cultured in the absence (-) or presence (+) of increasing testosterone concentration (T; 0.1-10 nM) for up to 72 h. (A-L) Representative wholemount images showing the developmental pattern of cultured ducts (n=6 animals/group from 3 different cultures).

600 Scale bar: 500 μm. (M) qPCR relative quantification of *Spag11c* and *Acta 2* mRNA in WDs cultured for 72 h with increasing testosterone concentrations, as indicated. Transcript levels were normalized using *Rpl19* as endogenous control and expressed in relation to organs cultured in the absence of testosterone. Values are mean ± SEM (n=5 animals/group). One-way ANOVA, followed by Bonferroni test; *$p < 0.05$.

605

Fig. 2. **Morphological differentiation and mRNA expression pattern of rat Wolffian duct (WD) cultured with testosterone and flutamide.** Morphological changes (A-P) and mRNA expression pattern (Q) in WDs collected at e17.5 and cultured in the absence (-) or presence (+) of 10 nM testosterone (T) and/or 10 μM flutamide (Flut) for up to 72 h. (A-T) Representative wholemount

610 images showing the developmental pattern of cultured ducts (n=10 animals/group from 5 different cultures). Scale bar: A-T, 500 μm. (Q) qPCR quantification of *Spag11c* and *Acta 2* mRNA in WDs cultured for 24 or 72 h in the absence or presence of testosterone and/or flutamide, as indicated. Transcript levels were normalized using *Rpl19* as endogenous control. The comparisons were made within each time-point (after 24 or 72 h of culture) and data expressed in relation to organs incubated in

615 the absence of testosterone. Values are mean ± SEM (n=3-5 animals/group). One-Way ANOVA followed by Tukey test; *$p < 0.05$.

Fig. 3. SPAG11C immunolocalization in freshly collected rat Wolffian duct (WD) and ducts cultured under different androgenic conditions. Comparison of the distribution pattern of SPAG11C immunoreactivity in freshly collected WD at e17.5 and e20.5 (A-B), as well as in e17.5 ducts cultured for 48 h or 72 h in the absence (-) or presence (+) of 10 nM testosterone (T) (G-J). ACTA2 immunostainings are also shown (D-E, K-N). Negative control consisted of primary antibody substituted by normal serum (C, F). Nuclei were stained with DAPI (blue). Results are representative of experiments performed in duplicate with tissues from 3 animals/group. WD epithelium, encircled with a white dashed line, is surrounded by the mesenchyme. Scale bar: A-F, 50 μm.

Fig. 4. SPAG11C immunolocalization in Wolffian duct (WD) from wild type (WT) and AR knockout (**ARKO) mice at e16.5.** Comparison of the SPAG11C immunodistribution pattern in WDs from WT (A-G) and ARKO (H-N) mice. Confocal fluorescence maximum projection images: B-G and I-N are higher magnification of the outlined areas in A and H. WD epithelium, encircled with a white dashed line, is surrounded by the mesenchyme in 2x confocal zoom-images (C, E, G, J, L, N). Note the mesenchymal cells (yellow arrows) directly surrounding the epithelium, which are characterized by absence/low intensity of SPAG11C immunoreactivity in WDs from WT mice (C, E, G). ACTA2 immunoreactivity, observed in the mesenchymal cells directly surrounding the epithelium of WD from WT (O) and ARKO (P) mice, was used as positive control. Negative control consisted of primary antibody substituted by normal serum (A – inset, Q). Nuclei were stained with DAPI (blue). Results are representative of experiments performed in duplicate with tissues from three mice/group. Testis (T), Wolffian duct (WD). Scale bars: A, H, 500 μm; B, D, F, I, K, M, O-Q, 50 μm.

Fig. 5. Effect of recombinant human SPAG11C (hSPAG11C) on the morphogenesis of the cultured Wolffian duct (WD). (A-I) Gross morphology of WDs cultured in the presence of

testosterone (T; 10 nM) and either bovine serum albumin (BSA; 80 nM; A-C) or hSPAG11C (80 nM; D-F). Recombinant hSPAG11C was washed out after 48 h of culture (G-I). Scale bar: A-I, 500 μm. Duct elongation (J) and coiling (K) was quantified after 72 h of culture. Values are mean ± SEM (n=5-12 animals/group from 3 different cultures). t test; ***$p<0.001$. (L-N) Number of proliferating epithelial cells in WDs cultured for 96 h was determined by immunofluorescence for phospho-histone H3. Representative image (objective 40x) of phospho-histone H3 immunofluorescence in organs incubated with BSA (L) or recombinant hSPAG11C (M). Nuclei were stained with DAPI (blue) and proliferating epithelial cells (red) were marked with yellow arrows. The number of phospho-histone H3-positive epithelial cells was expressed per mm of WD epithelium. Scale bar: L-M, 50 μm. Values are mean ± SEM (total of 6-7 microscope fields from 4 animals/group). t test, **$p<0.01$. (O-Q) Immunofluorescence with anti-his antibody showed hSPAG11C-positive staining in epithelial and mesenchymal cells of WDs 96 h-post incubation with recombinant hSPAG11C (P, Q), but not with BSA (O) (n=2 animals/group). Scale bar: O-Q, 500 μm.

Fig. S1. SPAG11C immunolocalization in rat Wolffian duct (WD) cultured with testosterone and flutamide. Comparison of the distribution pattern of SPAG11C immunoreactivity in e17.5 WDs cultured in the absence (-) or presence (+) of 10 nM testosterone (T) and/or 10 μM flutamide (Flut) for 72 h. Nuclei were stained with DAPI (blue). Results are representative of experiments performed in duplicate with tissues from 3 animals/group. Scale bar: A-F, 50 μm.

Fig. S2. Apoptosis in Wolffian duct (WD) cultured with recombinant human SPAG11C (hSPAG11C). Apoptosis was assessed by immunofluorescence for cleaved caspase-3 in WDs cultured with hSPAG11C (80 nM) or BSA for 96 h. Positive control consisted of immunostaining in bladder, which is a thicker tissue that was cultured together with WDs. Negative control consisted of primary

antibody substituted by normal rabbit serum. Results are representative of experiments performed in duplicate with tissues from 3 animals/group. Scale bar: A-D, 5O μm.

670 **Fig. S3. Comparison of *Spag11c* mRNA levels in Wolffian (WD) and Müllerian ducts (MD).** Values of *Spag11c* mRNA levels were normalized using *Rpl19* as endogenous control. Results were expressed in relation to WDs at e17.5. Values are mean ± SEM (n=3-4 animals/group). *p<0.05, Two-Way ANOVA followed by Bonferroni test; *p<0.05.
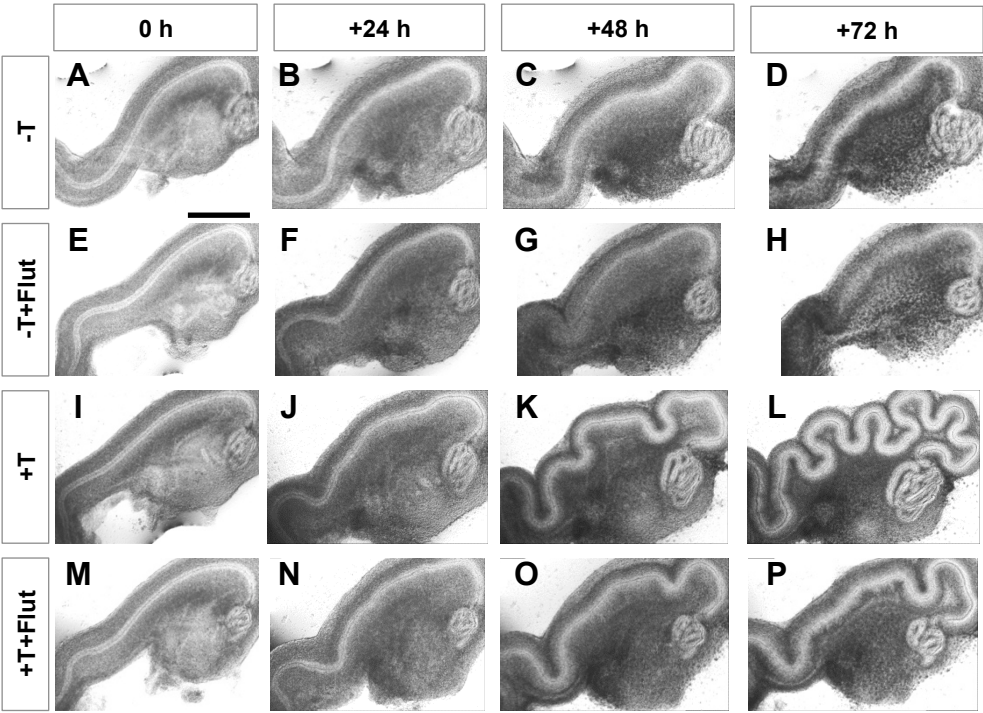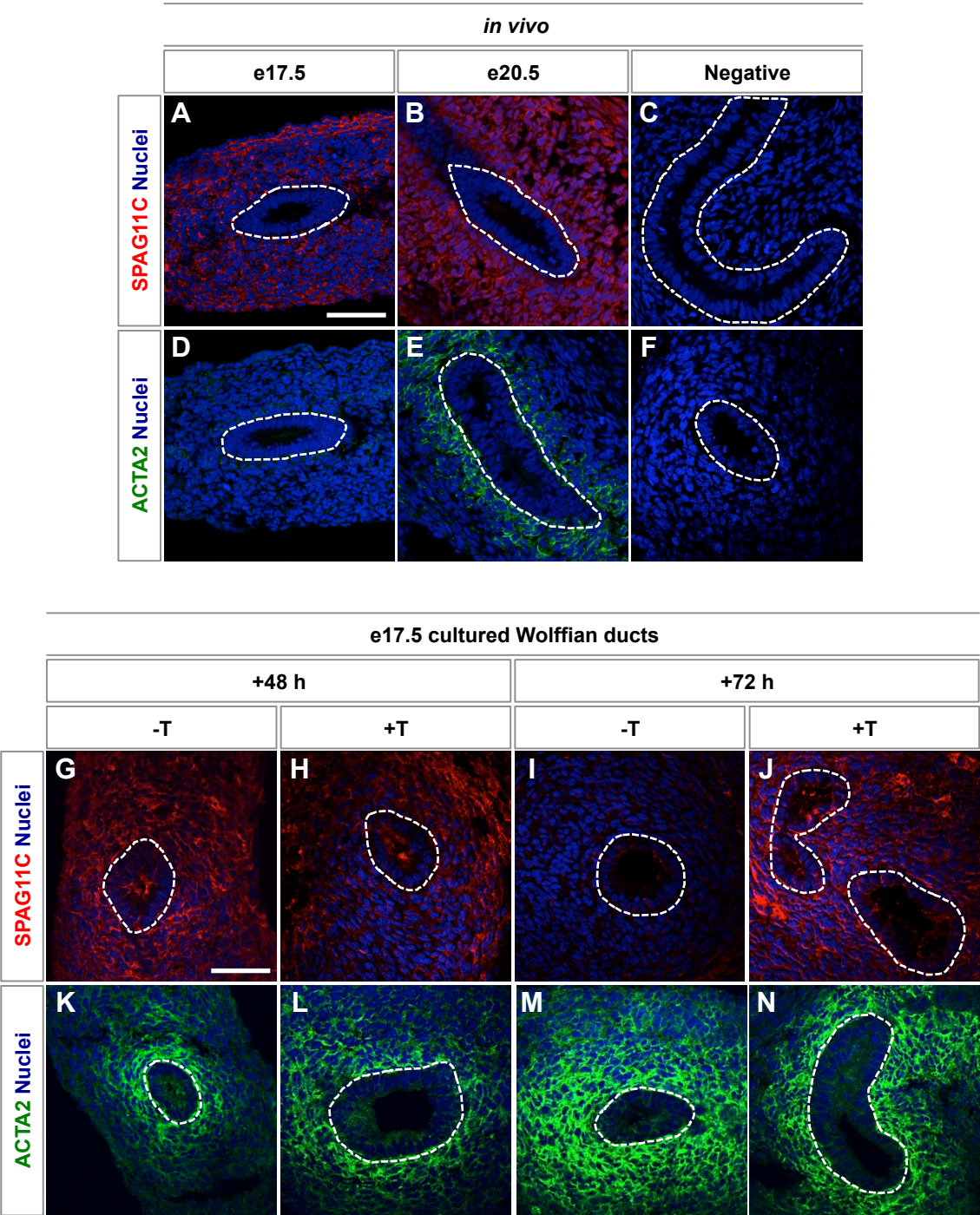
Fig. 1 – Ribeiro et al.
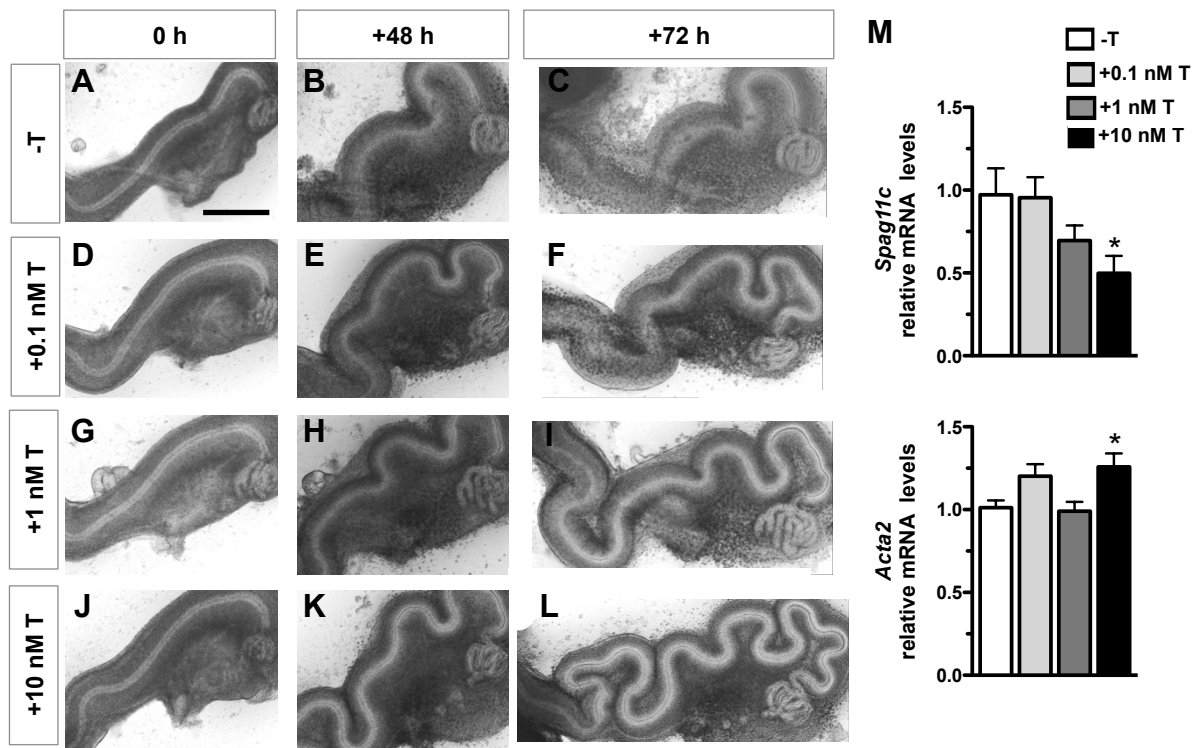
Fig. 2 – Ribeiro et al.
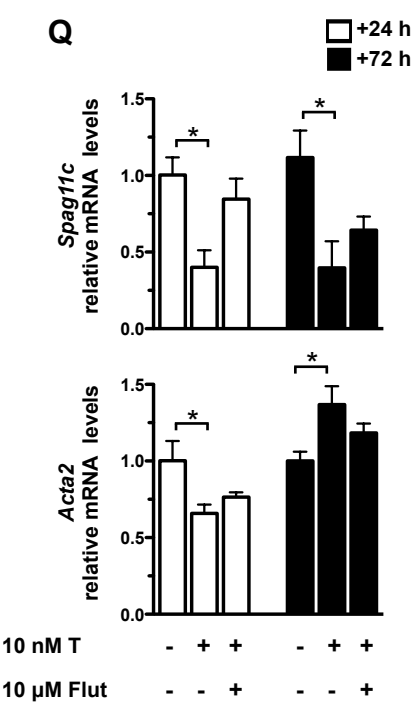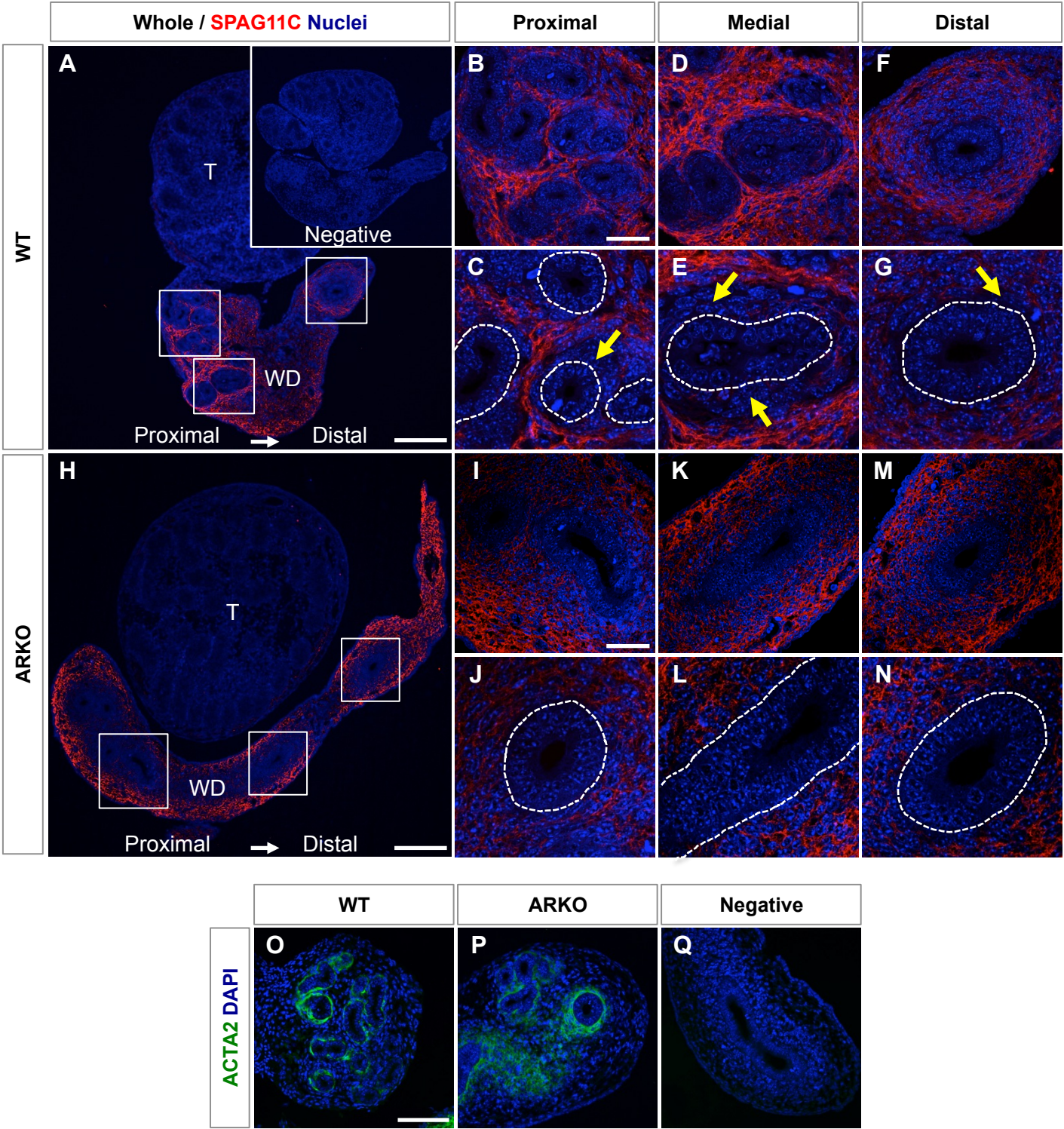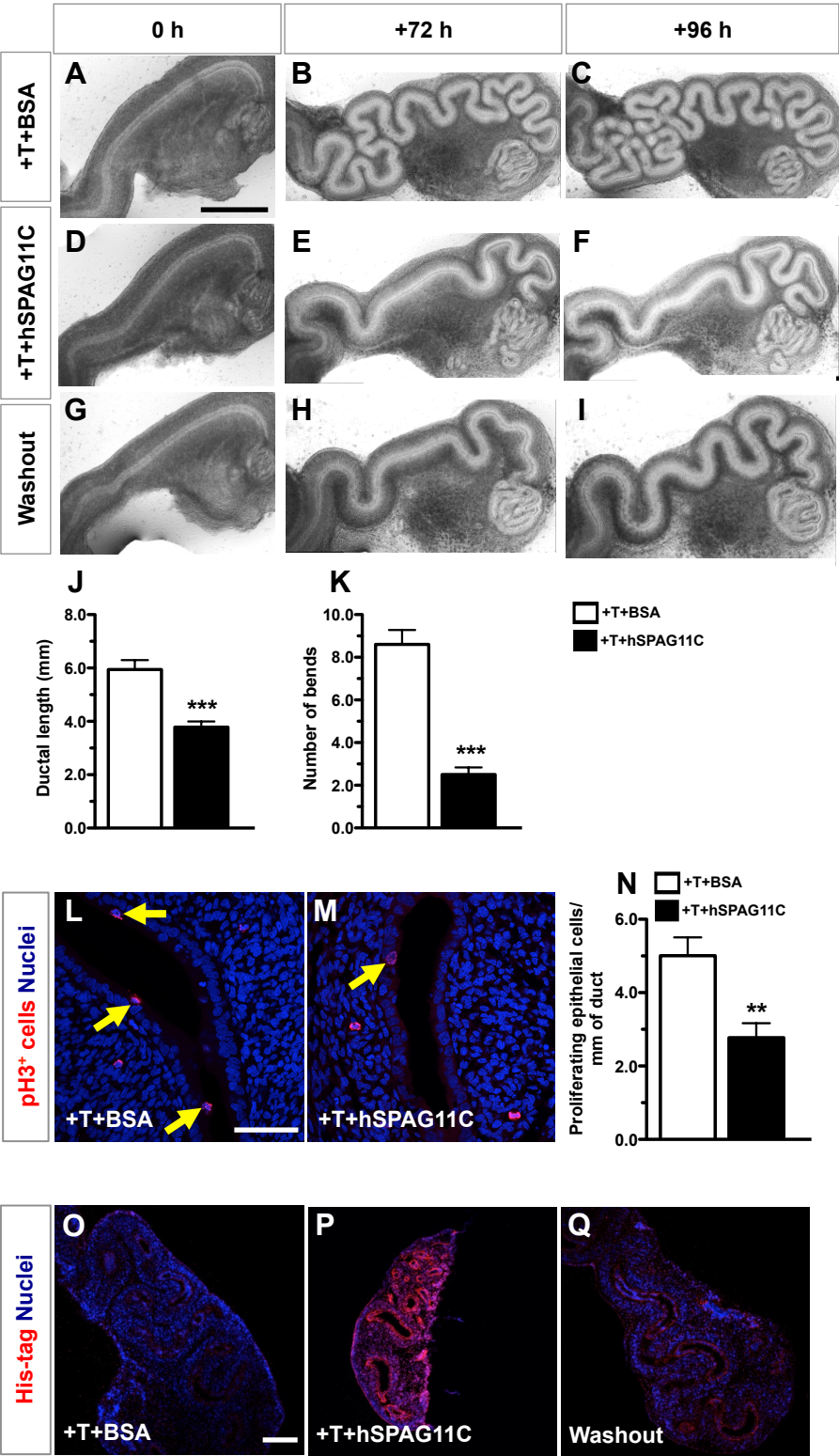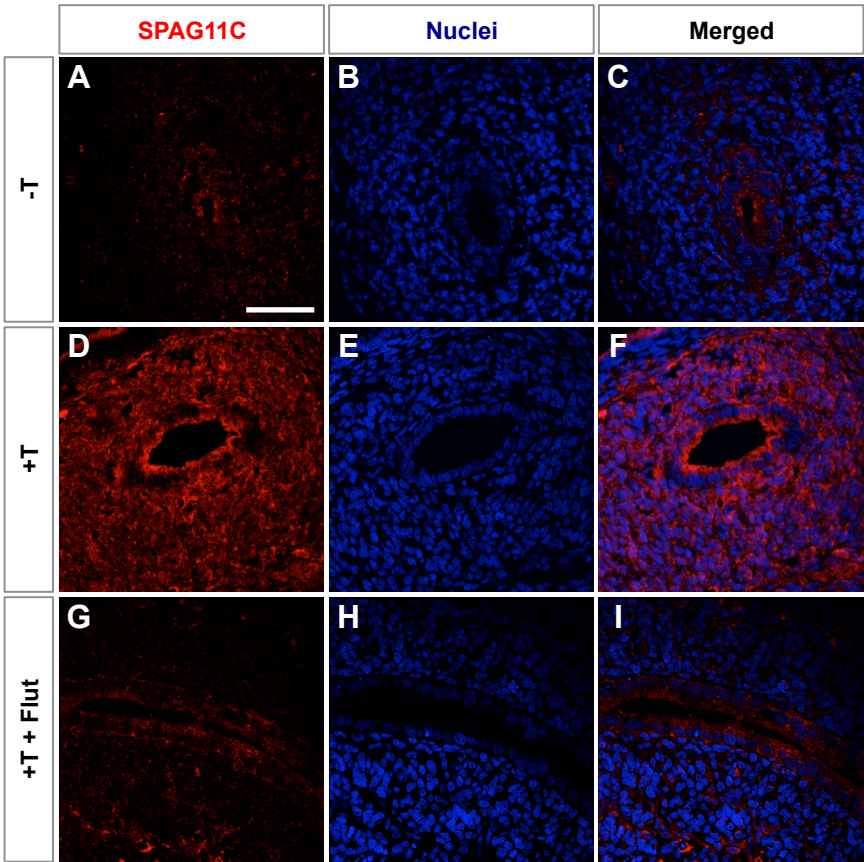
Fig. 3 – Ribeiro et al.

Fig. 4 – Ribeiro et al.
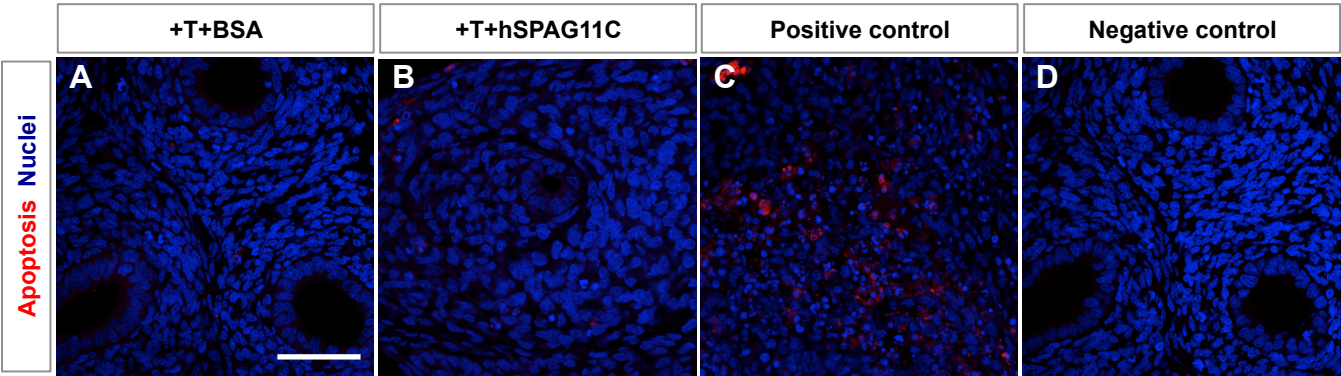

Whole / SPAG11C Nuclei	Proximal	Medial	Distal

WT

A · T · Negative · WD · Proximal → Distal

B · D · F

C · E · G

ARKO

H · T · WD · Proximal → Distal

I · K · M

J · L · N

WT	ARKO	Negative

ACTA2 DAPI

O · P · Q

Fig. 5 – Ribeiro et al.

Fig. S1 – Ribeiro et al.

	SPAG11C	Nuclei	Merged
-T	A	B	C
+T	D	E	F
+T + Flut	G	H	I

Fig. S2 – Ribeiro et al.

| +T+BSA | +T+hSPAG11C | Positive control | Negative control |

Fig. S3 – Ribeiro et al.